

# END TO END SIMULATIONS OF A NOVEL OPTICAL FIBRE MONITORING SYSTEM FOR ENERGY RECOVERY LINACs \*

A. Jones<sup>†,1</sup>, J. Wolfenden<sup>1</sup>, L. Eley<sup>1,2</sup>, C. P. Welsch<sup>1</sup>, University of Liverpool, Liverpool, UK

S. Boogert, Cockcroft Institute, Warrington, UK

<sup>1</sup>also at Cockcroft Institute, Warrington, UK

<sup>2</sup>also at Adaptix Ltd., Oxford, UK

## Abstract

Energy recovery LINACs (ERLs) are a type of novel accelerator, which recycle energy from old beams to new beams to increase machine energy efficiency. However, this can heighten beam instabilities, which limits the maximum beam current and increases beam losses. An optical fibre beam loss monitor (oBLM) can provide rapid and reliable beam loss monitoring, which is important for mitigating these instabilities. It obtains the beam loss location via time-of-flight analysis of Cherenkov radiation (CR) produced in optical fibres by relativistic particle showers from beam loss events. Operational demonstration of the oBLM system has previously been shown at several non-ERL facilities, but the multiple-energy, fast-repeating beams of ERLs present a unique challenge. Successful interpretation of ERL beam loss signals involves distinguishing losses from beams of different energies, which can be investigated through end-to-end Monte Carlo simulations of the radiation environment and its interaction with the oBLM system. This contribution presents Geant4 simulations of the oBLM response to sample sources of beam loss for beam energies of 7-500 MeV and bunch populations of  $(1\text{-}10) \times 10^6$  electrons.

## INTRODUCTION

Optical fibre-based beam loss monitors (oBLMs) consist of optical fibres running alongside a beamline, where at least one end of a fibre is monitored by a photodetector. oBLMs were first developed as a low-cost beam loss monitoring solution, with the capability for continuous accelerator coverage and better than 1 m precision in the reconstruction of beam loss locations [1-3].

Beam losses are detected through monitoring secondary particle showers from beam loss events, produced when high-energy beam particles strike an obstacle such as the inner wall of the beam pipe. The particle showers that intersect the optical fibre produce a pulse of Cherenkov radiation inside it [4] (Fig. 1). This radiation travels along the fibre and exits at the ends, where the photodetectors convert it into a voltage signal. The beam loss location can be reconstructed from the arrival time of the Cherenkov pulse [5]. A step-index silica fibre, with core diameter above 200  $\mu\text{m}$ , is one type of optical fibre that is effective for this purpose.

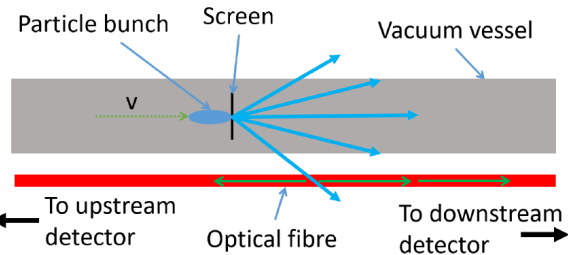


Figure 1: A diagram of the beam loss detection mechanism of the oBLM. Reproduced from [4] with permission.

Energy recovery LINACs (ERLs) are a type of novel accelerator in which the beam is returned to the RF cavities and decelerated after use, returning energy to the RF field and reducing the power consumption of the machine. However, the recirculating configuration necessary for ERLs leaves them at risk of high beam losses due to their unique susceptibilities to destabilising collective effects such as beam break-up [6] and the microbunching instability [7]. A beam loss monitor with continuous machine coverage, such as the oBLM, would provide useful data for diagnosing beam losses and managing collective effects across the whole length of an ERL.

The multiple recirculating beams present in ERLs pose a challenge for beam loss reconstruction with the oBLM.

ERL bunch properties, including their energy, can change significantly as they complete turns in the machine. Bunches that have made more turns (higher turn number) can be more susceptible to beam loss, since the effects of instabilities and slight variations from design specification can build up over time [8]. Therefore, it is important to have a method to determine the turn number of the bunch that produced a detected beam loss, as this can allow the losses of individual ERL bunches to be tracked throughout their full journey in the machine.

One potential method for this is through energy estimation of the bunch based on the recorded number of photons in the Cherenkov pulse. This is possible because the ERL bunch energy changes by a fixed value per turn, set by the energy gain or decrease from a single pass through the LINAC module(s) [9] - hence the bunch energy corresponds to its turn number. Also, the number of Cherenkov photons produced by a particle shower is expected to vary linearly with the energy of the shower-instigating particle [10] - so the bunch energy can, in principle, be estimated from the intensity of the oBLM Cherenkov signal. To aid distinguishing between

\* This work is supported by the Enhancing ERL development in the UK Grant (STFC ST/X000540/1) and the Cockcroft Institute Core Grant (STFC ST/V001612/1).

† sgajon11@liverpool.ac.uk

accelerating and decelerating bunches that have the same energy, this method can be augmented using a comparison of the photon detection time with the nominal bunch positions expected from the RF clock and the filling pattern [11], which allocates bunches into RF timing buckets based on their turn number.

However, the effect of the bunch energy must first be isolated from other influences on the oBLM signal, such as the number of lost particles (absolute loss intensity).

## SIMULATIONS

### Motivation for Simulations

The Cherenkov signal observed in an oBLM depends on the properties of the charge shower as it passes through the fibre; such as its energy, intensity, incidence angle, and time structure. The influences on these properties are difficult to estimate analytically: the initial properties of the shower depend on a combination of beam loss properties, such as beam energy and loss intensity [10]; and its ensuing evolution, such as attenuation by accelerator components and deflection in magnetic fields, depends on the specific component geometry, materials, and magnetic fields present around the beam loss location [12]. In light of this, it is simpler to investigate the expected oBLM signal by simulating the radiation environment with Monte Carlo tools.

### Preliminary Simulations in Geant4

Preliminary simulation studies of the oBLM system were conducted using the Geant4 [13–15] simulation program. These studies used a simplistic model: the beam was directed at a 1 cm-thick copper block to generate loss showers, with the fibre positioned outside a copper beam pipe (Fig. 2). The charged particles passing through the fibre were recorded, as were Cherenkov photons exiting the fibre ends. This model was successfully benchmarked against the results from a similar study [16] performed using the FLUKA code [17, 18].

To investigate the feasibility of bunch energy estimation using the oBLM signal, a  $5 \times 5$  grid search was performed over beam energies ( $E_{\text{beam}}$ ) of 7–500 MeV and absolute loss intensities ( $N_{\text{loss}}$ ) of 1–10 million particles – and the number of Cherenkov photons exiting the fibre ( $N_{\text{ph}}$ ) was recorded for each data point. The fibre was modelled with a 200  $\mu\text{m}$  core diameter and placed 45 cm from the beam axis (Fig. 2). The beam energy range was chosen to match that of the 6-turn configuration of the under-construction ERL PERLE (Powerful Energy Recovery LINAC for Experiments) [19], while the loss intensity was chosen to both ensure measurable photon statistics and manage run time constraints.

The grid search data was then plotted on a graph of  $N_{\text{ph}}$  against  $E_{\text{beam}}$  (with the data grouped by their value of  $N_{\text{loss}}$ ) and  $N_{\text{ph}}$  against  $N_{\text{loss}}$  (with the data grouped by their value of  $E_{\text{beam}}$ ). To estimate the approximate growth rate of  $N_{\text{ph}}$  with  $E_{\text{beam}}$  and  $N_{\text{loss}}$ , the gradients of straight-line fits to each grouped data set were compared.

This preliminary simulation method is similar to that of other simulation studies of optical fibre-Cherenkov detectors

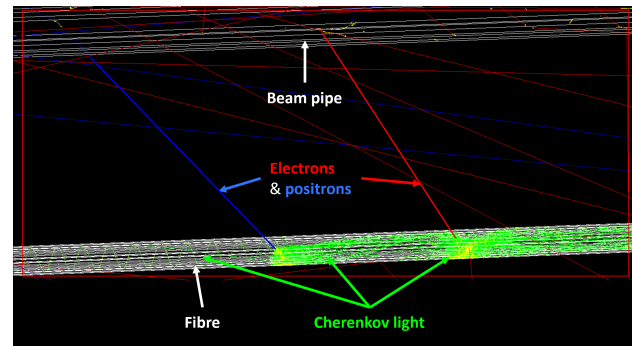


Figure 2: A section of simulation geometry used for preliminary studies, showing Cherenkov production & propagation in the fibre (Geant4 visualiser).

[1, 16, 20, 21], but it is computationally inefficient. The fibre covers a very small proportion of the angular region around the beam pipe, so only a similarly small minority of shower particles hit the fibre. The majority of particles miss, and are therefore considered wasted computing time.

### An Improved Simulation in BDSIM

To improve the computational efficiency of the simulation, a new model using a resampling method was developed using BDSIM (Beam Delivery Simulation) [22], a program based on Geant4.

In this method, beam losses are first simulated and the ensuing shower particles are recorded using a cylindrical sampling surface enclosing the accelerator model (Fig. 3). This produces a “loss map” of the particle showers at the radial distance from the design orbit immediately before the fibre (Fig. 4). For each particle passing the sampling surface, the curvilinear position  $s$ , azimuthal angle  $\phi$ , particle arrival time  $t$ , kinetic energy  $E_k$ , and momentum directions  $r'$ ,  $\phi'$ ,  $z'$  are recorded, along with the particle type. Next, a region of interest (ROI) is defined on the loss map as a band centred on the fibre position and ten times the width of the  $\phi$ -interval covered by the fibre width; representing the subset of shower particles with high likelihood to hit the fibre (approximately 0.7 mrad wide for a 200  $\mu\text{m}$ -core fibre at 45 cm from the beam). A Gaussian kernel density estimate (KDE) [23] is then used to resample a new set of particles with properties representative of the ROI. Finally, these new particles are simulated and the resulting Cherenkov photons they produce are recorded at the fibre ends.

This approach allows the fibre statistics to be increased while the beam loss shower evolves normally, as opposed to an alternative method of applying a physics bias to alter the angle of the showers to point towards the fibre. Additionally, this method produces a loss map of the accelerator, which is helpful for understanding the evolution of the beam loss showers.

The usage of BDSIM also brings the advantage of a machine-agnostic simulation: BDSIM can generate a representative simulation geometry from a MAD-X TFS twiss

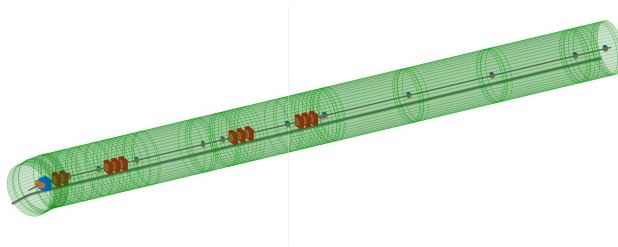


Figure 3: The simulated model of CLEAR (CERN Linear Electron Accelerator for Research), generated from a MAD-X survey file of the accelerator [24,25], visualised in BDSIM. The sampling surface (green) is displayed, and a fibre model can be seen running alongside the beam pipe (fibre enlarged for clarity). The beam travels from right to left.

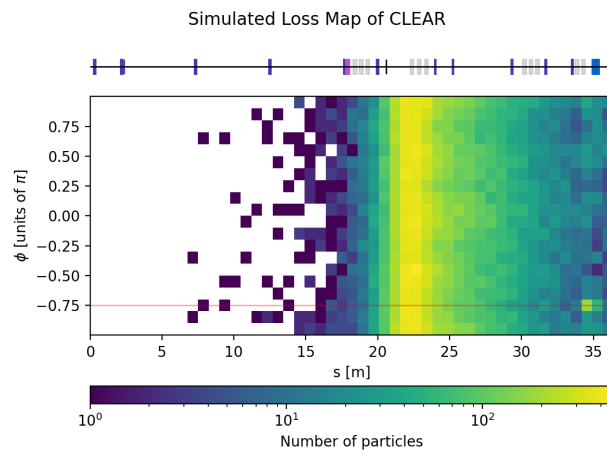


Figure 4: Loss map histogram in  $s$  and  $\phi$  of the CLEAR model from Fig. 3, generated from a screen inserted at 20.6 m. The ROI is displayed in red, and the simulated machine layout is shown above the graph<sup>1</sup>.

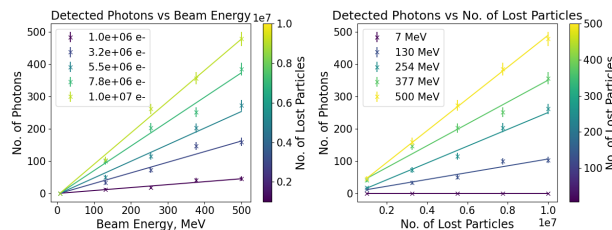


Figure 5: Parameter scan data of  $N_{ph}$  against  $E_{beam}$  (left) and  $N_{loss}$  (right), from the preliminary simulations. Straight-line fits are shown for each data set.

file (Fig. 3), enabling the simulation to be applied to any accelerator with a MAD-X model.

The resampling simulation code was developed using a basic testing model consisting of twenty quadrupoles, a sector dipole, and a copper screen inserted after the second cell to generate beam losses.

<sup>1</sup> Note: In Fig. 4,  $\phi = 0.5\pi$  corresponds to the outside curve of the dipole.

## RESULTS

The results from the preliminary simulations are shown in Fig. 5. The expected linear trends appeared, as shown by the straight line fits for each data set, but there is some fluctuation around the expected result. Despite the low photon statistics, the mean uncertainty on the gradient values is approximately 6.5 % - acceptable for a preliminary study.

The gradients of  $N_{ph}$  against  $E_{beam}$  ranged from  $(0.9\text{--}9.7) \times 10^{-1}$  MeV $^{-1}$  - four orders of magnitude greater than the  $(1.1\text{--}4.9) \times 10^{-5}$  range measured for the gradients of  $N_{ph}$  against  $N_{loss}$ . This suggests the effect of beam energy can dominate the signal and the energy estimation method is feasible, but only if the absolute loss intensity varies by less than 4 orders of magnitude.

An example loss map histogram from the new simulation method is displayed in Fig. 4, comprising over 48,000 charged shower particles generated from 20,000 220 MeV input beam particles. The beam loss appears approximately uniform in  $\phi$ , aside from a small beam loss hotspot in the lower-right of the image around  $\phi = -0.75\pi$ . Hence, the ROI and fibre are positioned over this spot in order to maximise the detected beam loss signal.

The working principle of the resampling simulation was also demonstrated in the basic testing model, with 50 initial beam loss particles, over 5000 loss map detections, and  $10^4$  resampled particles.

## CONCLUSION

Preliminary simulations of the fibre-Cherenkov response to varying beam energies suggest that energy estimation of a bunch from the Cherenkov signal intensity is feasible, but only if the absolute loss intensity varies by less than 4 orders of magnitude. However, since even small particle bunches such as 1 pC contain over  $6 \times 10^6$  particles, the loss intensity can vary over a much greater range than four orders of magnitude in practice. The energy estimation method is therefore best supported by an alternative means of estimating the absolute loss intensity, such as an ionisation chamber BLM placed in a key beam loss region.

The working principle of the BDSim simulation has also been demonstrated in the basic testing model, and a loss map was recorded from a model of the CLEAR accelerator has been generated using its MAD-X survey file. However, further work is required for full demonstration of the simulation principle with the CLEAR model, such as adapting the resampling methods to handle larger quantities of particle shower data. The simulation will also be verified against experimental oBLM data recorded on CLEAR in April 2025, the success of which would enable further testing on models of ERL machines such as PERLE.

## REFERENCES

[1] M. Kastriotou, “Optimisation of storage rings and RF accelerators via advanced fibre-based detectors”, Ph.D. thesis, Dept. of Physics, University of Liverpool, Liverpool, May 2018. <https://livrepository.liverpool.ac.uk/3033777>

[2] E. Janata and M. Körfer, “Radiation detection by Cerenkov emission in optical fibers at TTF”, Flash, DESY, Hamburg, Germany, Rep. TESLA-2000-27, Dec. 2000. [https://flash.desy.de/reports\\_publications/tesla\\_reports/tesla\\_reports\\_2000/](https://flash.desy.de/reports_publications/tesla_reports/tesla_reports_2000/)

[3] A. Intermite, M. Putignano, and C. P. Welsch, “Feasibility Study of an optical fibre sensor for beam loss detection based on a SPAD array”, in *Proc. DIPAC'09*, Basel, Switzerland, May 2009, pp. 228–230. <https://jacow.org/d09/papers/TUPB27.pdf>

[4] J. Wolfenden *et al.*, “Cherenkov radiation in optical fibres as a versatile machine protection system in particle accelerators”, *Sensors*, vol. 23, no. 4, p. 2248, Jan. 2023. [doi:10.3390/s23042248](https://doi.org/10.3390/s23042248)

[5] S. Benítez Berrocal *et al.*, “Beam loss localisation with an optical beam loss monitor in the CLEAR facility at CERN”, in *Proc. IPAC'22*, Bangkok, Thailand, Jun. 2022, pp. 351–354. [doi:10.18429/JACoW-IPAC2022-MOPOT045](https://doi.org/10.18429/JACoW-IPAC2022-MOPOT045)

[6] G. H. Hoffstaetter and I. V. Bazarov, “Beam-breakup instability theory for energy recovery linacs”, *Phys. Rev. Spec. Top. Accel. Beams*, vol. 7, no. 5, p. 054401, May 2004. [doi:10.1103/PhysRevSTAB.7.054401](https://doi.org/10.1103/PhysRevSTAB.7.054401)

[7] Z. Huang *et al.*, “Suppression of microbunching instability in the linac coherent light source”, *Phys. Rev. Spec. Top. Accel. Beams*, vol. 7, no. 7, p. 074401, Jul. 2004. [doi:10.1103/PhysRevSTAB.7.074401](https://doi.org/10.1103/PhysRevSTAB.7.074401)

[8] A. Bartnik *et al.*, “CBETA: First Multipass Superconducting Linear Accelerator with Energy Recovery”, *Phys. Rev. Lett.*, vol. 125, no. 4, p. 044803, Jul. 2020. [doi:10.1103/PhysRevLett.125.044803](https://doi.org/10.1103/PhysRevLett.125.044803)

[9] S. A. Bogacz *et al.*, “Beam dynamics driven design of powerful energy recovery linac for experiments”, *Phys. Rev. Accel. Beams*, vol. 27, no. 3, p. 031603, Mar. 2024. [doi:10.1103/PhysRevAccelBeams.27.031603](https://doi.org/10.1103/PhysRevAccelBeams.27.031603)

[10] P. Gorodetzky *et al.*, “Quartz fiber calorimetry”, *Nucl. Instrum. Methods Phys. Res. A*, vol. 361, no. 1, pp. 161–179, Jul. 1995. [doi:10.1016/0168-9002\(95\)00295-2](https://doi.org/10.1016/0168-9002(95)00295-2)

[11] S. Setiniyaz, R. Apsimon, and P. H. Williams, “Filling pattern dependence of regenerative beam breakup instability in energy recovery linacs”, *Phys. Rev. Accel. Beams*, vol. 24, no. 6, p. 061003, Jun. 2021. [doi:10.1103/PhysRevAccelBeams.24.061003](https://doi.org/10.1103/PhysRevAccelBeams.24.061003)

[12] S. L. Kramer, V. J. Ghosh, M. Breitfeller, and W. Wahl, “Shielding NSLS-II light source: Importance of geometry for calculating radiation levels from beam losses”, *Nucl. Instrum. Methods Phys. Res. A*, vol. 835, pp. 13–33, Nov. 2016. [doi:10.1016/j.nima.2016.08.017](https://doi.org/10.1016/j.nima.2016.08.017)

[13] S. Agostinelli *et al.*, “Geant4—a simulation toolkit”, *Nucl. Instrum. Methods Phys. Res. A*, vol. 506, no. 3, pp. 250–303, 2003. [doi:10.1016/S0168-9002\(03\)01368-8](https://doi.org/10.1016/S0168-9002(03)01368-8)

[14] J. Allison *et al.*, “Geant4 developments and applications”, *IEEE Trans. Nucl. Sci.*, vol. 53, no. 1, pp. 270–278, Feb. 2006. [doi:10.1109/TNS.2006.869826](https://doi.org/10.1109/TNS.2006.869826)

[15] J. Allison *et al.*, “Recent developments in Geant4”, *Nucl. Instrum. Methods Phys. Res. A*, vol. 835, pp. 186–225, Nov. 2016. [doi:10.1016/j.nima.2016.06.125](https://doi.org/10.1016/j.nima.2016.06.125)

[16] M. King *et al.*, “A systematic investigation of beam losses and position-reconstruction techniques measured with a novel oBLM at CLEAR”, *Instruments*, vol. 9, no. 1, p. 4, Mar. 2025. [doi:10.3390/instruments9010004](https://doi.org/10.3390/instruments9010004)

[17] CERN, Home | The official CERN FLUKA website, <https://fluka.cern/>

[18] G. Battistoni *et al.*, “Overview of the FLUKA code”, *Ann. Nucl. Energy*, vol. 82, pp. 10–18, Aug. 2015. [doi:10.1016/j.anucene.2014.11.007](https://doi.org/10.1016/j.anucene.2014.11.007)

[19] D. Angal-Kalinin *et al.*, “PERLE: Powerful Energy Recovery Linac for Experiments - conceptual design report”, *J. Phys. G*, vol. 45, no. 6, p. 065003, Jun. 2018. [doi:10.1088/1361-6471/aaa171](https://doi.org/10.1088/1361-6471/aaa171)

[20] S. Benítez, B. Salvachúa, and M. Chen, “Beam loss detection based on generation of Cherenkov light in optical fibers in the CERN Linear Electron Accelerator for Research”, *Phys. Rev. Accel. Beams*, vol. 27, no. 5, p. 052901, May 2024. [doi:10.1103/PhysRevAccelBeams.27.052901](https://doi.org/10.1103/PhysRevAccelBeams.27.052901)

[21] M. Santana-Leitner *et al.*, “Monte Carlo Optimization of Fast Beam Loss Monitors for LCLS-II”, in *Proc. IPAC'19*, Melbourne, Australia, May 2019, pp. 4066–4069. [doi:10.18429/JACoW-IPAC2019-THPRB102](https://doi.org/10.18429/JACoW-IPAC2019-THPRB102)

[22] L. J. Nevay *et al.*, “BDSIM: An accelerator tracking code with particle-matter interactions”, *Comput. Phys. Commun.*, vol. 252, p. 107200, Jul. 2020. [doi:10.1016/j.cpc.2020.107200](https://doi.org/10.1016/j.cpc.2020.107200)

[23] T. Hastie, R. Tibshirani, and J. Friedman, “Kernel smoothing methods”, in *The Elements of Statistical Learning: Data Mining, Inference, and Prediction*, T. Hastie, R. Tibshirani, and J. Friedman, Eds. New York, NY: Springer New York, NY, 2009, pp. 191–218. [doi:10.1007/978-0-387-84858-7\\_6](https://doi.org/10.1007/978-0-387-84858-7_6)

[24] K. N. Sjobak *et al.*, “Status of the CLEAR Electron Beam User Facility at CERN”, in *Proc. IPAC'19*, Melbourne, Australia, May 2019, pp. 983–986. [doi:10.18429/JACoW-IPAC2019-MOPTS054](https://doi.org/10.18429/JACoW-IPAC2019-MOPTS054)

[25] CLEAR, acc-models / acc-models-clear · GitLab, Apr. 2023, <https://gitlab.cern.ch/acc-models/acc-models-clear>